

The Photon Content of the Neutron

Keping Xie

Michigan State University

DPF-Pheno 2024

May 14, 2024

In collaboration with

Tim J. Hobbs (ANL) and Bei Zhou (Fermilab)

[JHEP 04 \(2024\) 022 \[arXiv:2305.10497\]](#)

Motivations

The neutron structure

- We have entered the precision era for the proton structure [\[2203.13923\]](#).
- How about the neutron?
- Isospin-symmetry to relate the neutron's quark-gluon PDFs.
- To what precision this isospin symmetry is preserved?
- Many **isospin symmetry violation** sources: **QED interaction**, nuclear effects.

Phenomenological relevance

- Nucleus scattering
- Neutrino-nucleus scattering: W production
- Photon initiated processes: photonic Axion-like particle production

Recall the proton's photon PDFs

The first generation

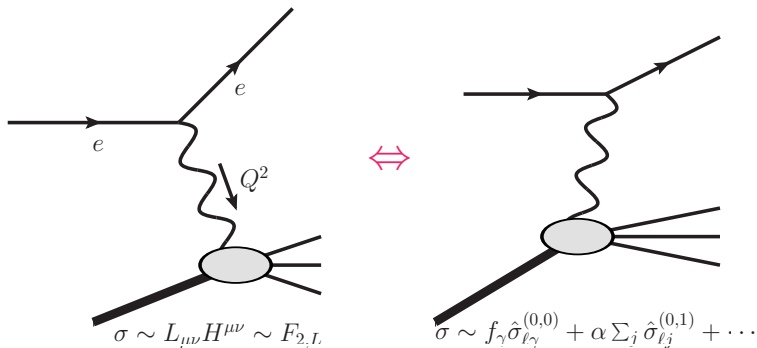
- **MRST2004QED** [0411040] models the photon PDF with an effective mass scale.
- **NNPDF23QED** [1308.0598] and **NNPDF3.0QED** [1410.8849] constrains photon PDF with the LHC Drell-Yan data, $q\bar{q}, \gamma\gamma \rightarrow \ell^+\ell^-$
- **CT14qed_inc** fits the inelastic ZEUS $ep \rightarrow e\gamma + X$ data [1509.02905], and include elastic component as well.

The second generation

- **LUXqed** directly takes the structure functions $F_{2,L}(x, Q^2)$ to constrain photon PDF uncertainty down to percent level [1607.04266,1708.01256]
- **NNPDF3.1luxqed** [1712.07053] initializes photon PDF with LUX formula at $\mu_0 = 100$ GeV (a high scale) and evolves DGLAP equation both upwardly and downwardly.
- **MMHT2015qed** [1907.02750] initializes photon at red $\mu_0 = 1$ GeV (a low scale) and evolve DGLAP upwardly. It's updated as **MSHT20qed** by the recent fit [2111.05357].
- **CT18qed** [2305.10733] incorporates the LUX formalism with the CT18 [1912.10053] global analysis.

The LUX formalism

- The DIS process: $ep \rightarrow e + X$



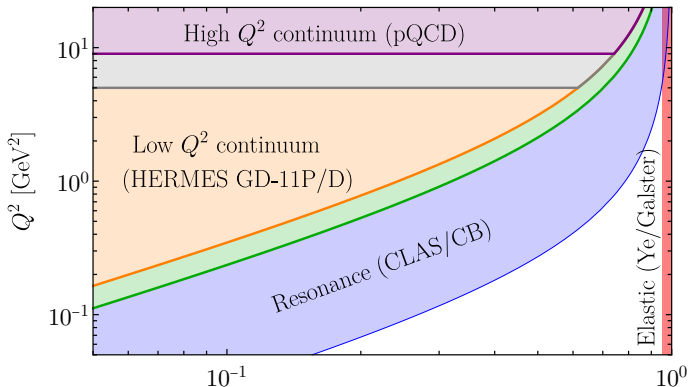
- Matching these two approaches leads to the LUX master formula ^[1607.04266,1708.01256]

$$x\gamma(x, \mu^2) = \frac{1}{2\pi\alpha(\mu^2)} \int_x^1 \frac{dz}{z} \left\{ \int_{\frac{x^2 m_p^2}{1-z}}^{\frac{\mu^2}{1-z}} \frac{dQ^2}{Q^2} \alpha_{\text{ph}}^2(-Q^2) \left[\left(z p_{\gamma q}(z) + \frac{2x^2 m_q^2}{Q^2} \right) \times \right. \right. \\ \left. \left. F_2(x/z, Q^2) - z^2 F_L(x/z, Q^2) \right] - \alpha^2(\mu^2) z^2 F_2(x/z, \mu^2) \right\}.$$

The square bracket term corresponds to the “**physical factorization**” scheme, while the second term is referred as the “ **$\overline{\text{MS}}$ -conversion**” term.

- The structure functions $F_{2,L}$ can be directly measured, or calculated through pQCD in the high-energy regime.

Breakup of (x, Q^2) plane



- In the resonance region $W^2 = m_p^2 + Q^2(1/x - 1) < W_{\text{lo}}^2 = 3 \text{ GeV}^2$, the structure functions are taken from CLAS [0301204] or Christy-Bosted [0712.3731] fits.
- In the low- Q^2 continuum region $W^2 > W_{\text{hi}}^2 = 4 \text{ GeV}^2$, the HERMES GD11-P [1103.5704] fits with ALLM [PLB1991] functional form.
- In the high- Q^2 region ($Q^2 > Q_{\text{PDF}}^2$), $F_{2,L}$ are determined through pQCD.
- The elastic form factors are taken from A1 [1307.6227] or Ye [1707.09063] fits of world data.

All these ingredients can be applied to neutron as well.

Electromagnetic form factors

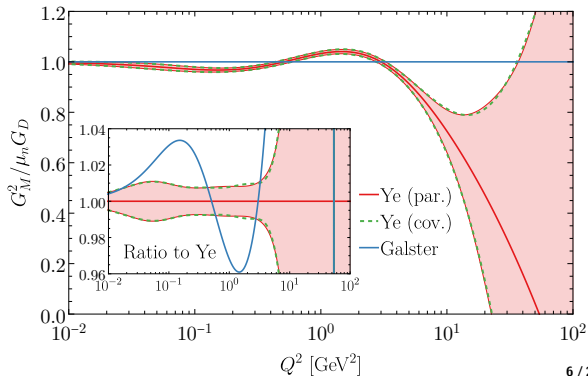
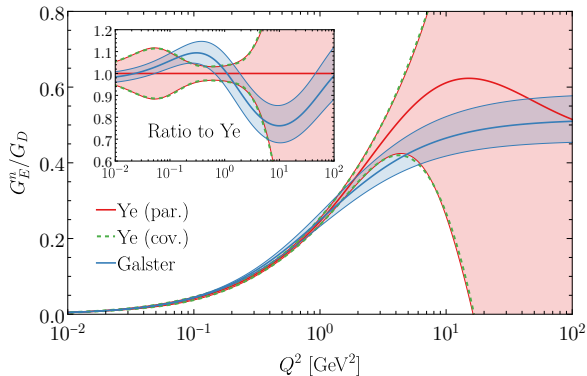
- Galster parameterization [NPB1971]

$$G_E^n(Q^2) = \frac{A\tau}{1+B\tau} G_D(Q^2), \quad G_D(Q^2) = 1/(1+Q^2/\Lambda^2)^2,$$

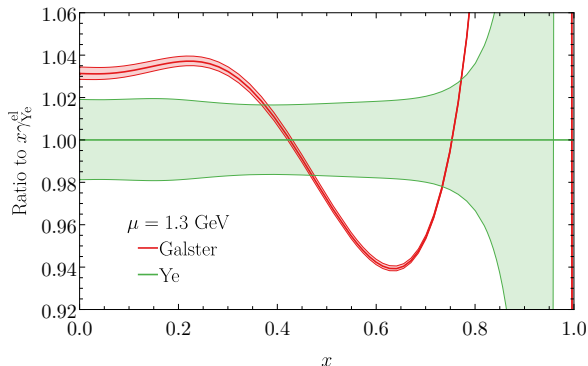
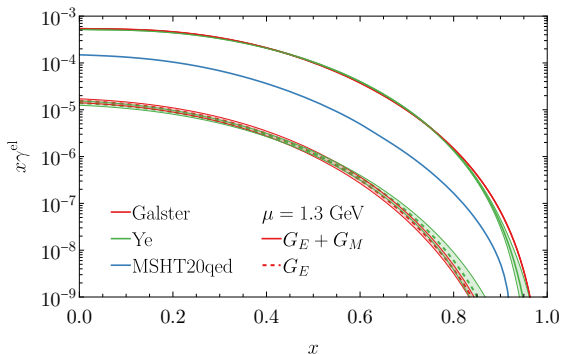
where [Kelly, PRC2004]

$$A = 1.70 \pm 0.04, \quad B = 3.30 \pm 0.32$$

- Modern fit from world electron scattering data: Extracted from nuclei (e.g., D, He) [Ye et al., 1707.09063]

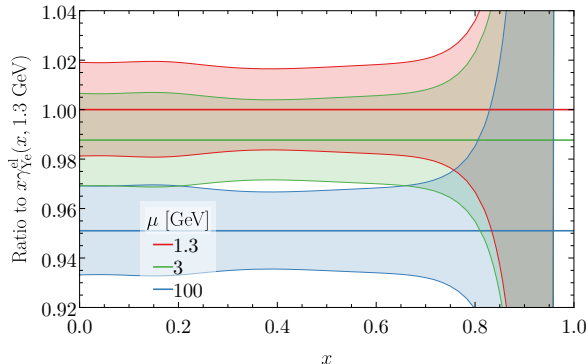
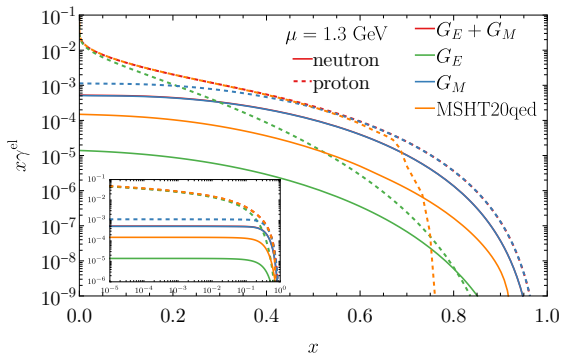


Elastic photon



- Neutron's elastic photon mainly comes from the magnetic form factor G_M
- Consistent with the zero electric charge
- MSHT20qed integrate elastic form factor up to 1 GeV and then evolve to high scale.
- We take the complete integration to $Q^2 \rightarrow \infty$, while scale dependence comes from the running coupling $\alpha(\mu^2)$.

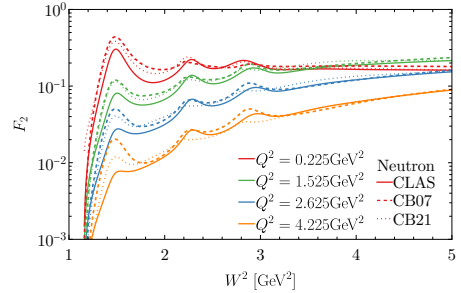
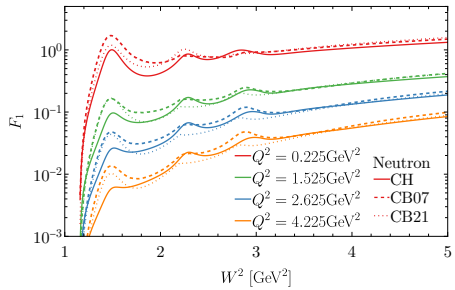
In comparison proton's elastic photon



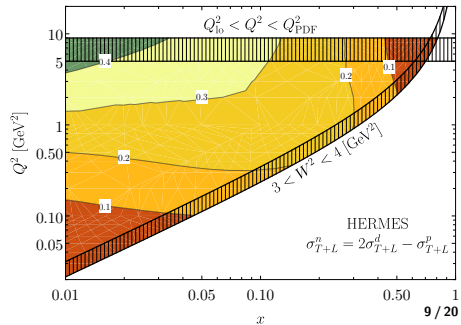
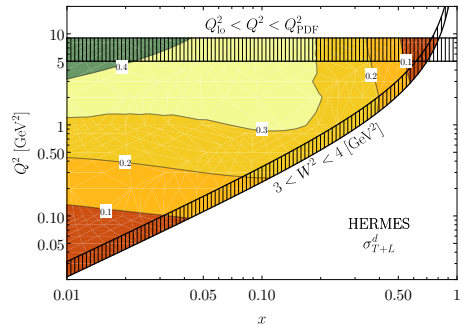
- In comparison, the proton's elastic photon is consistent with each other, except at large x due to the numerical interpolation issue.
- The proton's low- x elastic photon mainly comes from the G_E , while large- x from G_M .
- The elastic photon decrease with scale, due to $\alpha(\mu^2)$ running.

Neutron non-perturbative structure functions

Resonance:
 CLAS [0301204]
 Christy-Bosted
 [0712.3731,0711.0159]



Low- Q^2 continuum:
 HERMES [1103.5704]



A smooth transition

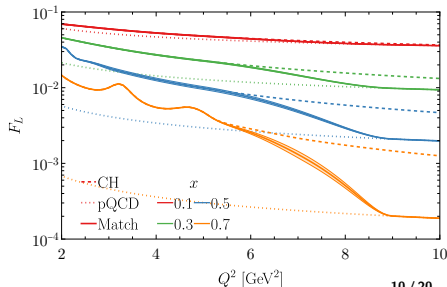
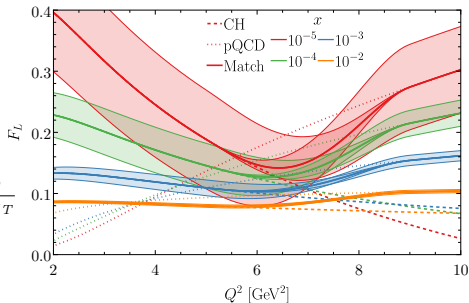
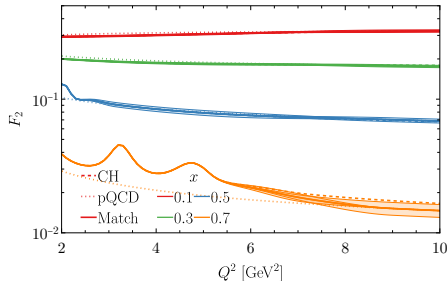
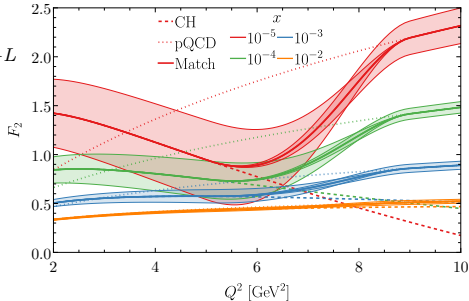
$$F_2 = \frac{1}{4\pi^2\alpha} \frac{Q^2(1-x)}{1+4x^2m^2/Q^2} \sigma_{T+L}$$

- At moderate x , HERMES can match pQCD very well.
- Large uncertainty for HERMES low- x extrapolation
- Extreme x transit to the resonance region $W^2 = Q^2(1/x - 1)$

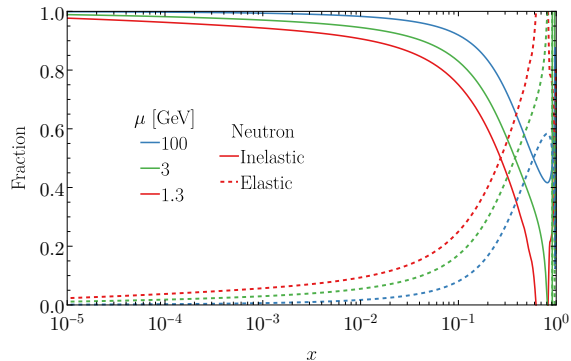
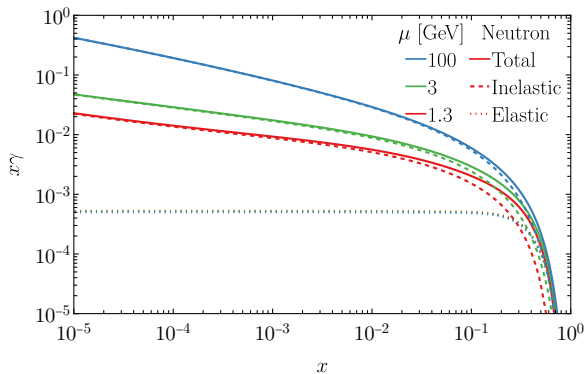
$$F_L = \left(1 + \frac{4m^2x^2}{Q^2}\right) F_2 \frac{R_{L/T}}{1+R_{L/T}}$$

$$R_{L/T} = R_{1998}(1 \pm 50\%)$$

[9808028]

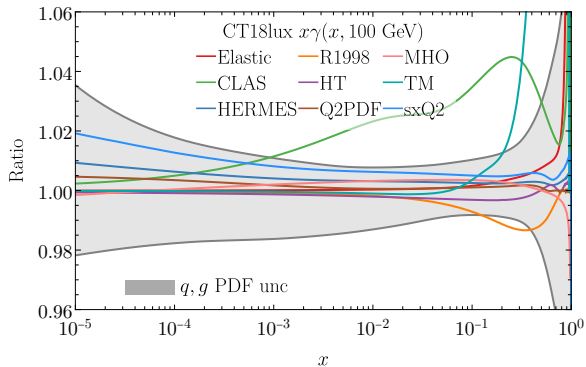
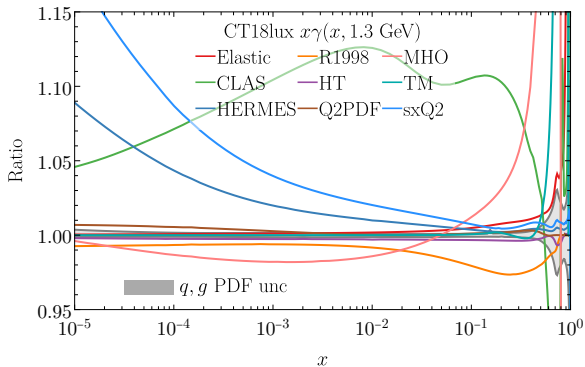


Inelastic photon



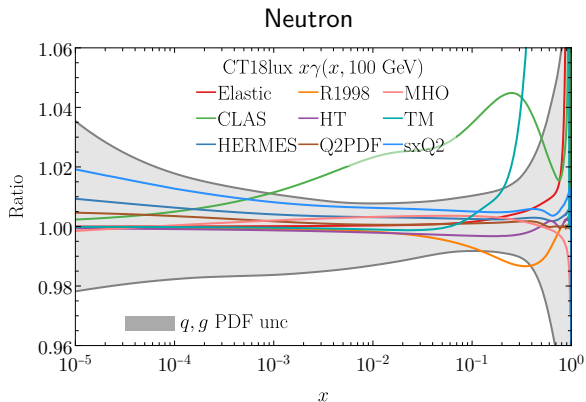
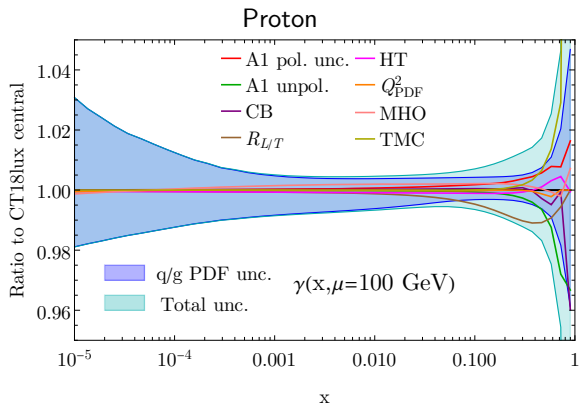
- The inelastic photon dominates.
- Elastic photon (mainly from G_M) only become relevant at very large x ($\gtrsim 0.2$)
- Inelastic photon evolves very fast

Non-perturbative uncertainties



- The resonance variation dominates at low Q^2
- The low- Q^2 non-perturbative uncertainty dies out with increasing scale, while pQCD (q, g PDF) uncertainty increase.
- Non-perturbative uncertainties remain at large x

In comparison with proton



- The proton's photon PDF uncertainty is about 1% level.
- The neutron's photon is (2 ~ 4)% in the moderate- x region.
- A significant improvement in comparison with the 1st generation of photon PDFs.

Isospin symmetry violation

Inspired by MSHT20qed

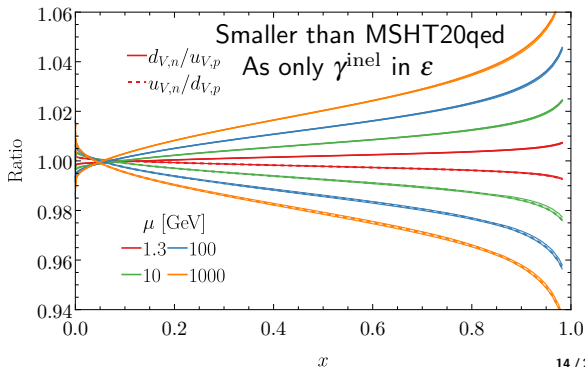
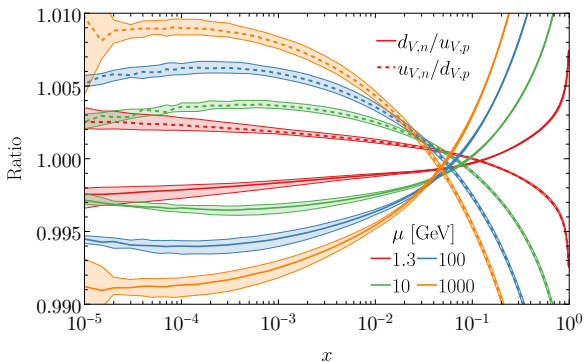
- Model the initial isospin violation with QED interaction

$$\varepsilon = \frac{\int dx x (\gamma_p^{\text{inel}}(x, \mu_0^2) - \gamma_n^{\text{inel}}(x, \mu_0^2))}{\int dx x \left(\frac{3}{4} u_{V,p}^{(\text{QED})}(x, \mu_0^2) - 3 d_{V,p}^{(\text{QED})}(x, \mu_0^2) \right)}$$

$$\Delta d_{V,n}(x, \mu_0^2) = d_{V,n}(x, \mu_0^2) - u_{V,p}(x, \mu_0^2) = \varepsilon \left(1 - \frac{e_d^2}{e_u^2} \right) u_{V,p}^{(\text{QED})}(x, \mu_0^2),$$

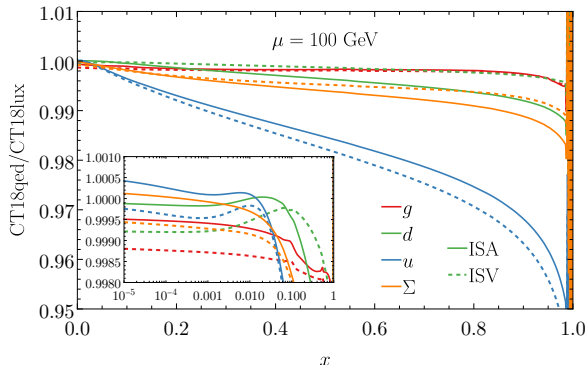
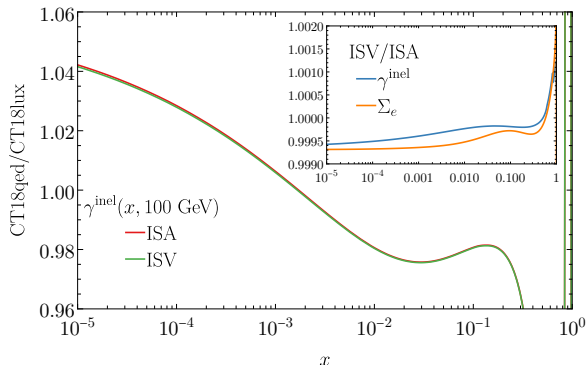
$$\Delta u_{V,n}(x, \mu_0^2) = u_{V,n}(x, \mu_0^2) - d_{V,p}(x, \mu_0^2) = \varepsilon \left(1 - \frac{e_u^2}{e_d^2} \right) d_{V,p}^{(\text{QED})}(x, \mu_0^2).$$

- The ε parameter can be self-consistently determined through sum rules.

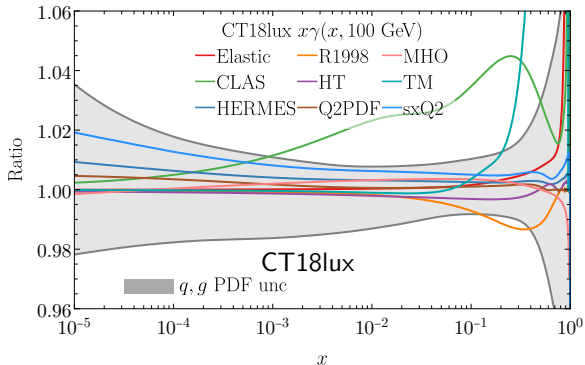
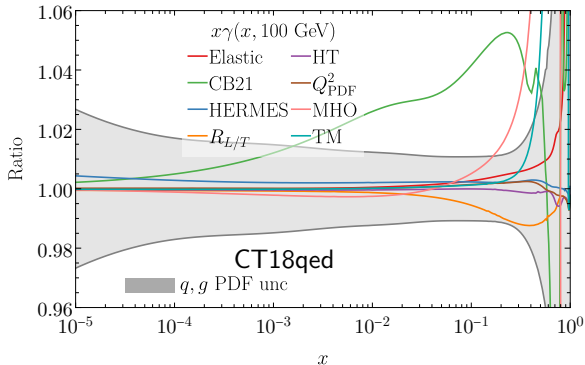


LUX vs DGLAP

- CT18lux: directly calculate the photon PDF with the **LUX** formalism
- CT18qed: initialize the inelastic photon PDF with the LUX formalism at low scales, and evolve the $\text{QED}_{\text{NLO}} \otimes \text{QCD}_{\text{NNLO}}$ **DGLAP** equations up to high scales, similar to MMHT2015qed/MSHT20qed.
- CT18qed gives larger low- x photon due the evolution: $\int d \log \mu^2 \frac{\alpha}{2\pi} \sum_q e_q^2 x P_{\gamma q} \otimes xq \sim F_2^{\text{LO}} > F_2^{\text{NNLO}}$
- Photon radiation take away the quark fraction at large x .

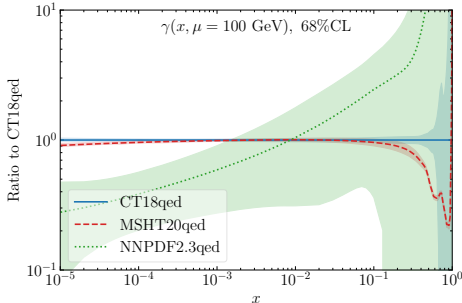
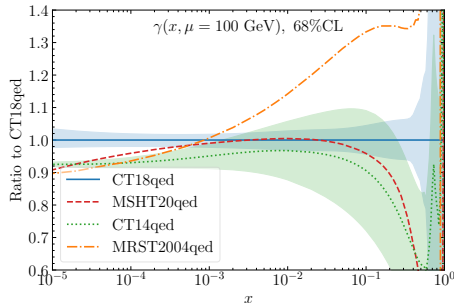
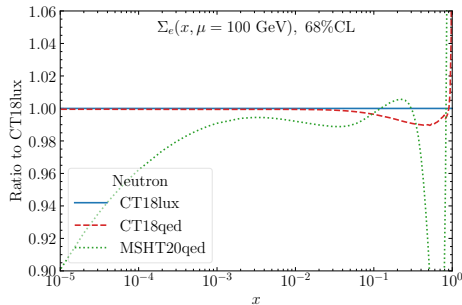
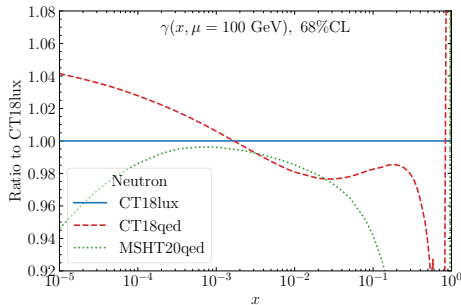


CT18qed uncertainties



- Uncertainty consistent with the CT18lux
- The resonance uncertainty slightly increases, while the low- Q^2 non-perturbative uncertainty improves.
- The iso-spin symmetry violation effect on the photon PDF as well as the momentum sum rule is minimal.

In comparison with other PDFs



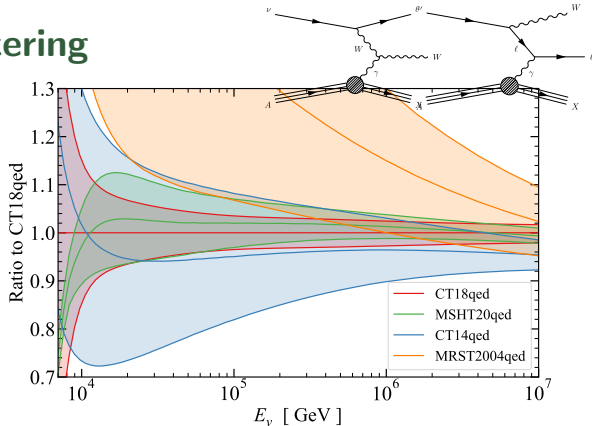
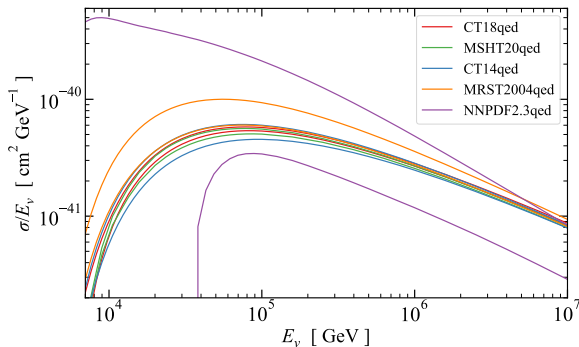
- Similarly to the proton case, CT18qed consistent with MSHT20qed at moderate x

- Low- x photon is driven by the charge weighted singlet Σ_e

- The large- x is driven by both Σ_e and non-perturbative treatment.

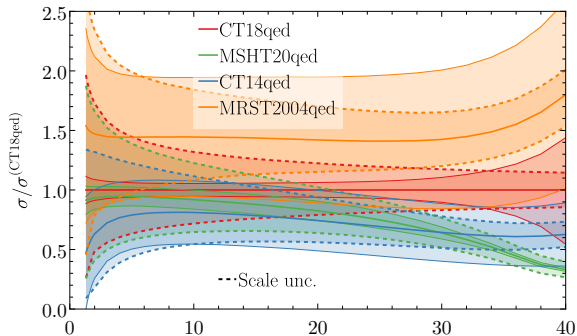
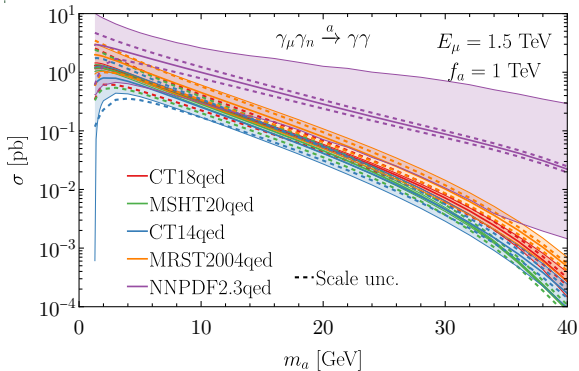
- Improvement with respect to 1st generation 17 / 20

W boson production in ν - A scattering



- W -boson production can be measured at in high-energy neutrino telescopes, e.g., IceCube, KM3NET, as well as collider, *i.e.*, FASER and future FPFs
- Our photon PDF directly contributes to the photon-initiated sub-process
- The photon PDF uncertainty is reduced to a percent level.

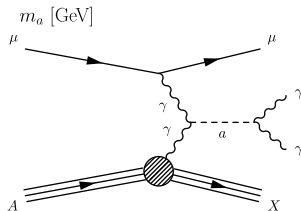
Axion-like particle production



- A similar mechanism applies to photonic Axion-like particle production.
- For simplicity, we demonstrate it with the muon beam dump experiment

$$E_\mu = 1.5 \text{ TeV}, \sqrt{s} = \sqrt{2E_\mu m_N} = 53 \text{ GeV}.$$

- Many PDF features remain the same.



Conclusion

CT18qed is available: <http://cteq-tea.gitlab.io/project/00pdfs/>

- The neutron's photon content can be precisely determined by mapping the structure functions to the PDF, the LUXqed formalism.
- The elastic photon comes from the electromagnetic form factors.
- The inelastic component comes from inelastic structure functions.
- We divide the (x, Q^2) into three regions: the resonance, low- Q^2 continuum, and high- Q^2 pQCD regions.
- Similarly to the proton case, we explored two methods, LUX vs DGLAP, which give CT18lux and CT18qed, respectively. Both are consistent with each other.
- The photon PDF precision is significantly improved, with respect to the 1st generation PDFs.
- CT18qed is consistent with MHST20qed in the moderate- x region. Discrepancies were found in the low- x and large- x regions, driven by the corresponding charge-weighted singlet as well as non-perturbative treatments.
- Phenomenological implications explored with the W -boson production in the νA scattering and the photonic ALP production.
- Some future directions can be continued, such as nuclear corrections.